Grounding Zone mapping in Antarctica using radar interferometry

L. Charrier[1], B. Scheuchl[1], J. Mouginot[2], S. Jeong[1], V. Brancato[1,3], E. Rignot[1,3]

[1]University of California, Irvine, Irvine USA.

[2]Institut des Géosciences de l'Environnement, Grenoble, France.

[3]Jet Propulsion Laboratory, Pasadena, USA

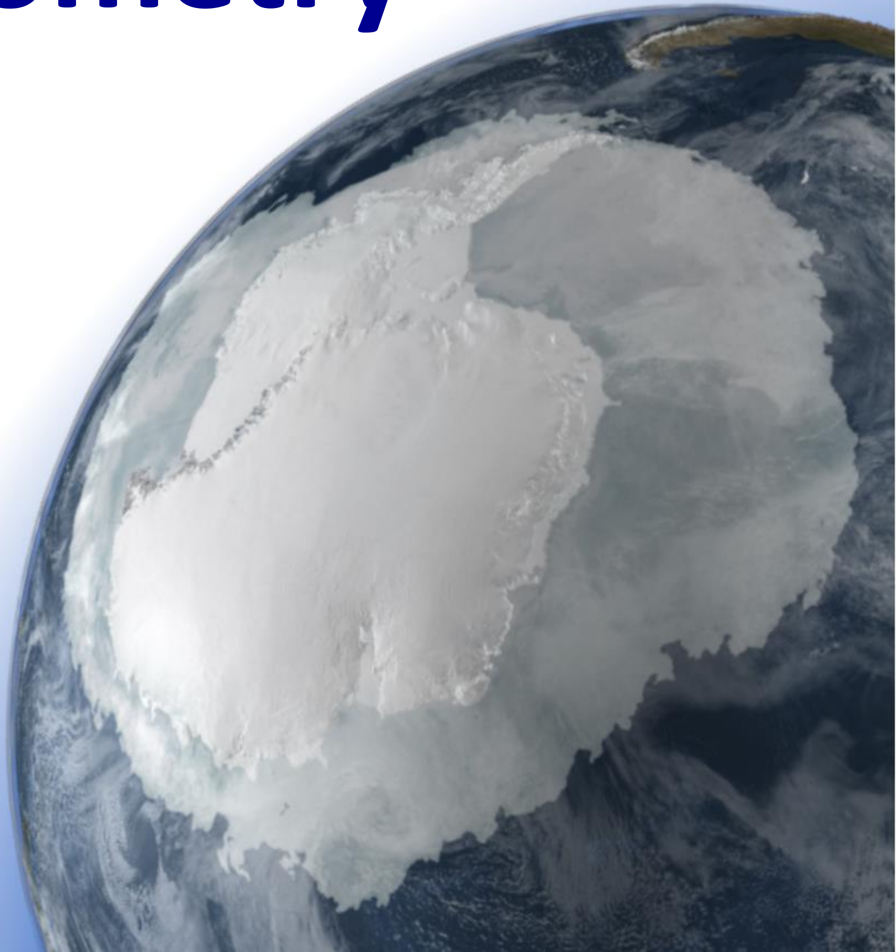

Ice-sheet melt contributes to sea-level rise (SLR)

=> Still a lot of uncertainties in projecting future SLR

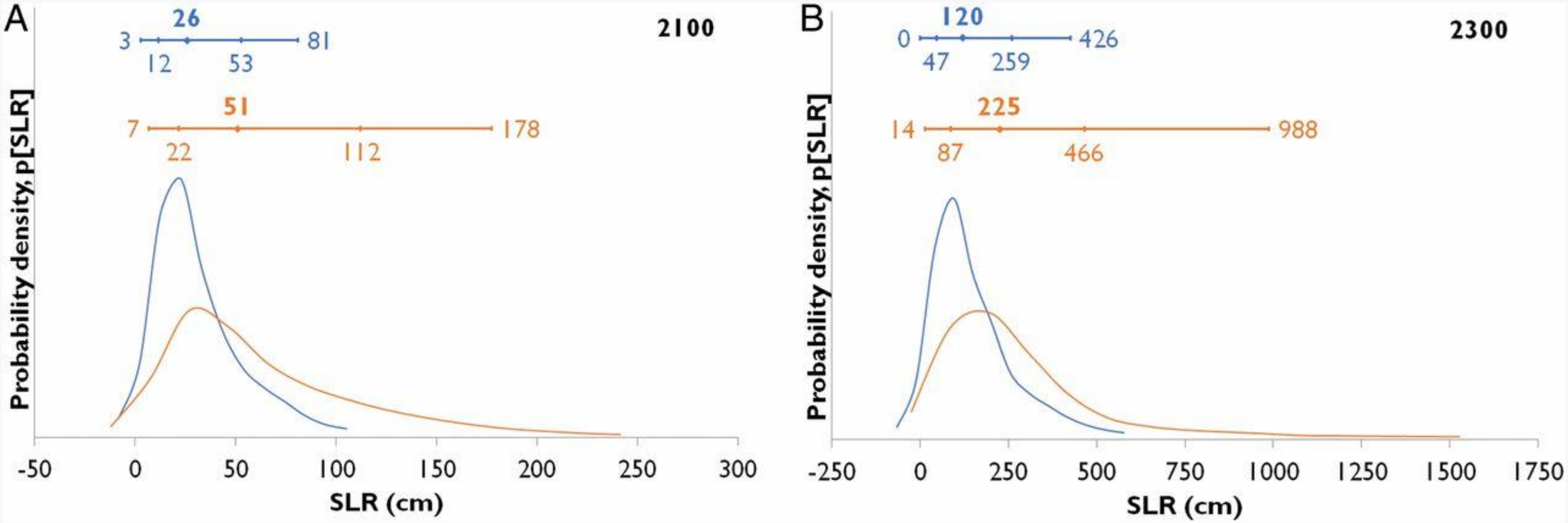

Probability Distribution functions for a +2°C temperature scenario (blue) and +5°C temperature scenario (red) temperature scenarios for the combined ice sheet SLR contributions at (A) 2100 and (B) 2300.
Bamber et al., 2019

Grounding line (GL) : a crucial feature

To know accurately GL position:

- To constrain numerical models
  - Grounded ice = basal friction
  - Floating ice = zero friction
- To detect retreat and advances of glaciers
- To compute ice-sheet mass balance
  - Ice thickness is much lower downstream of the GL

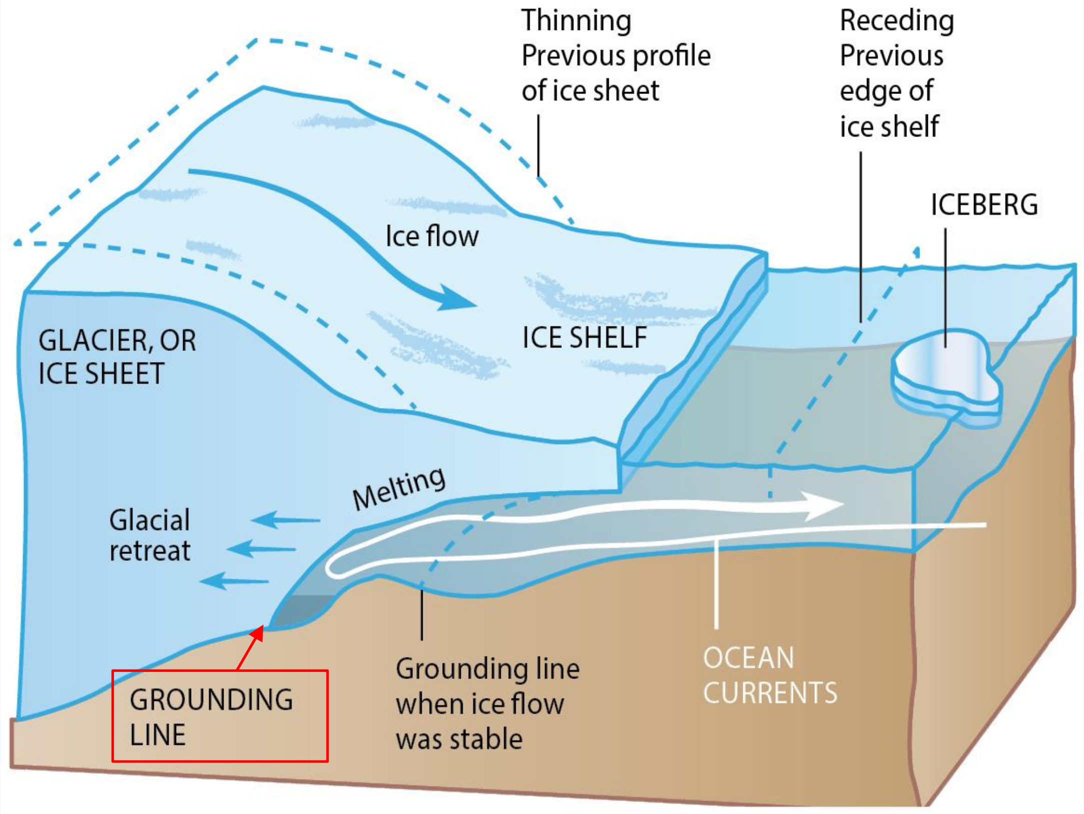

L. Charrier, B. Scheuchl, J. Mouginot, S. Jeong, V. Brancato, E. Rignot

Sentinel-1: a higher temporal resolution

Double difference interferometry = current state of the art way

Traditional approach (few available acquisitions):
→ A grounding line

Today (ongoing observations):
→ A grounding zone (short-term grounding line migration)

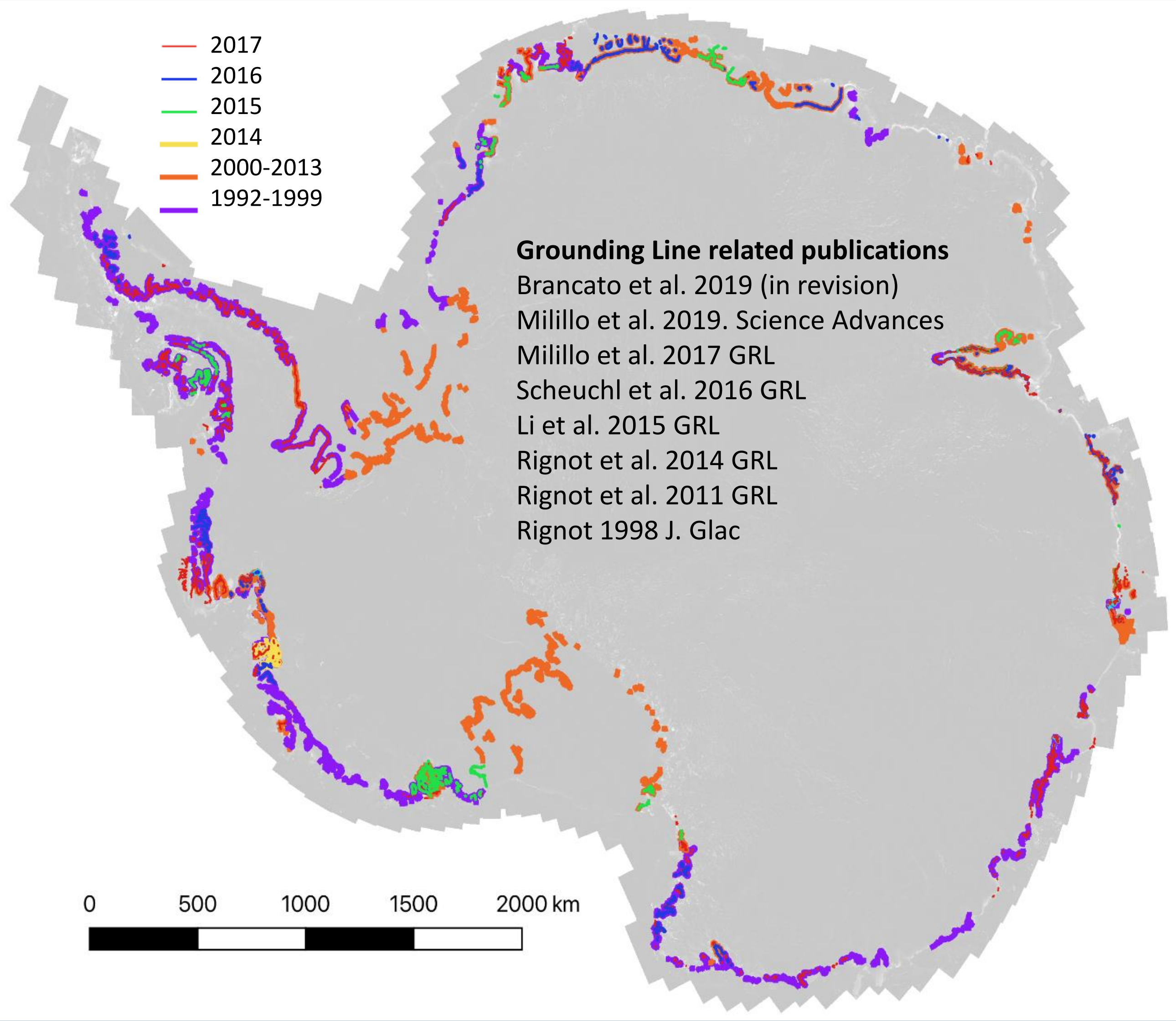

Objectives/Research questions

- Provide an update to grounding line position in Antarctica

- What is the range of the short-term variations of the grounding line?

- How to explain these variations?

- What is the long-term variation of grounding line position taking into account these new data?

Study Area

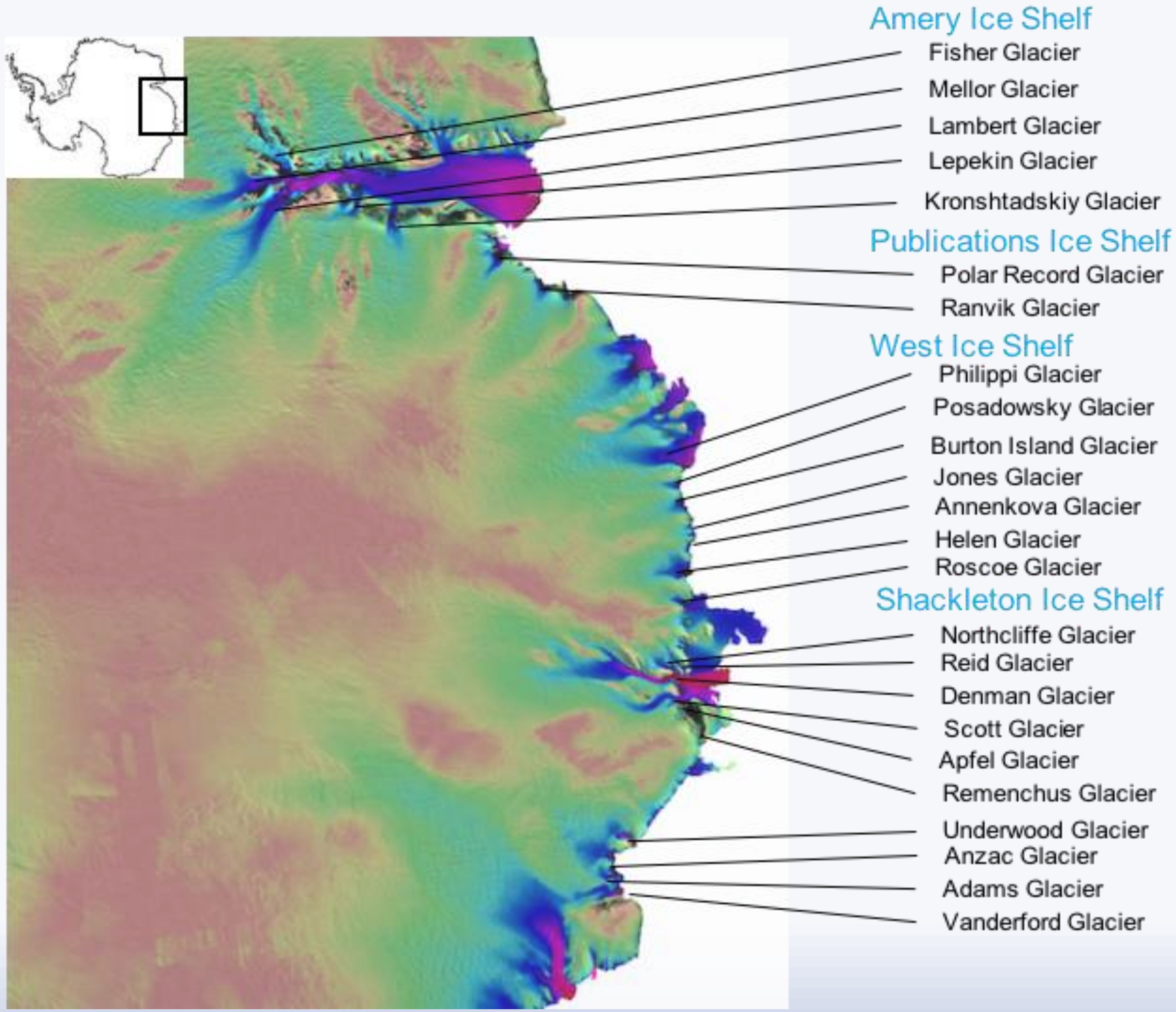

L. Charrier, B. Scheuchl, J. Mouginot, S. Jeong, V. Brancato, E. Rignot

Grounding line position detection

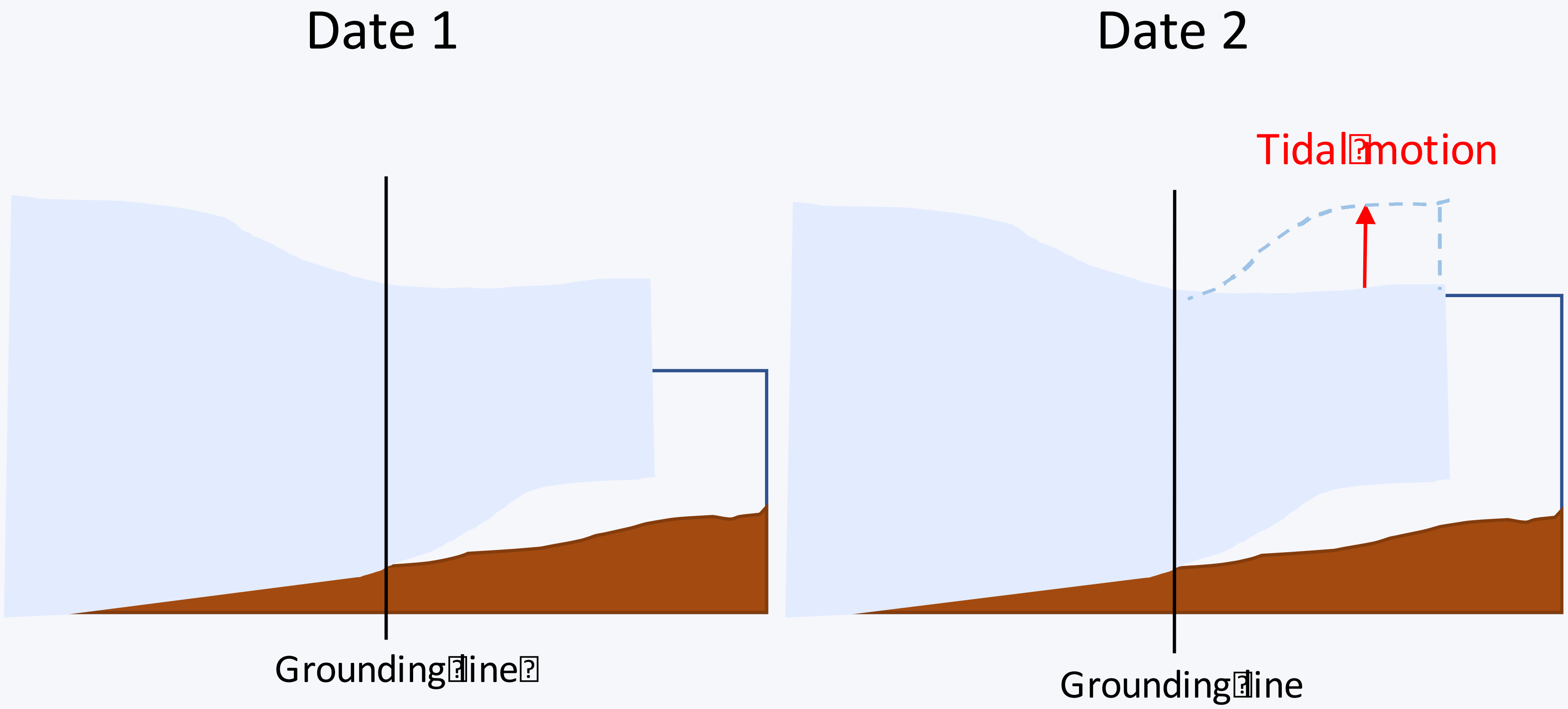

InSAR method

SAR $\phi = \frac{4\pi}{\lambda} r_1 + \phi_{ground} + \phi_{noise}\ [2\pi]$

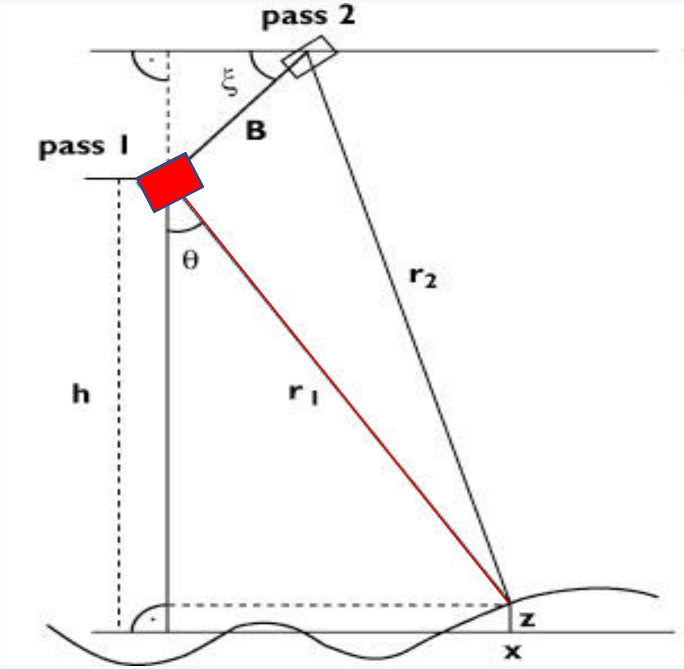

InSAR method

SAR

$$\phi = \underbrace{\frac{4\pi}{\lambda} r_1 + \phi_{ground} + \phi_{noise}}_{\text{unknown}} \ [2\pi]$$

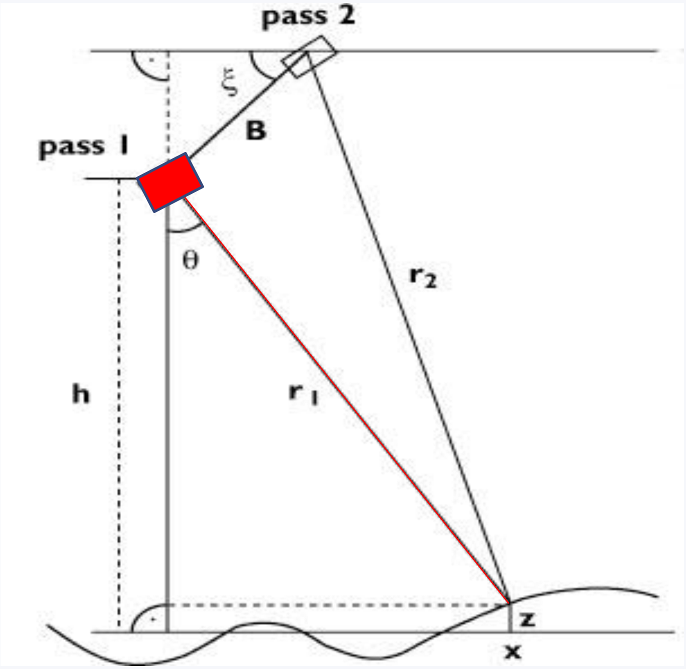

InSAR method

SAR $\phi = \frac{4\pi}{\lambda} r_1 + \phi_{ground} + \phi_{noise}\ [2\pi]$

InSAR $\Delta\phi = \frac{4\pi}{\lambda}\left(r_1 - r_2 + \cancel{\phi_{ground}}_1 - \cancel{\phi_{ground}}_2 + \phi_{noise\ 1} - \phi_{noise\ 2}\right)\ [2\pi]$

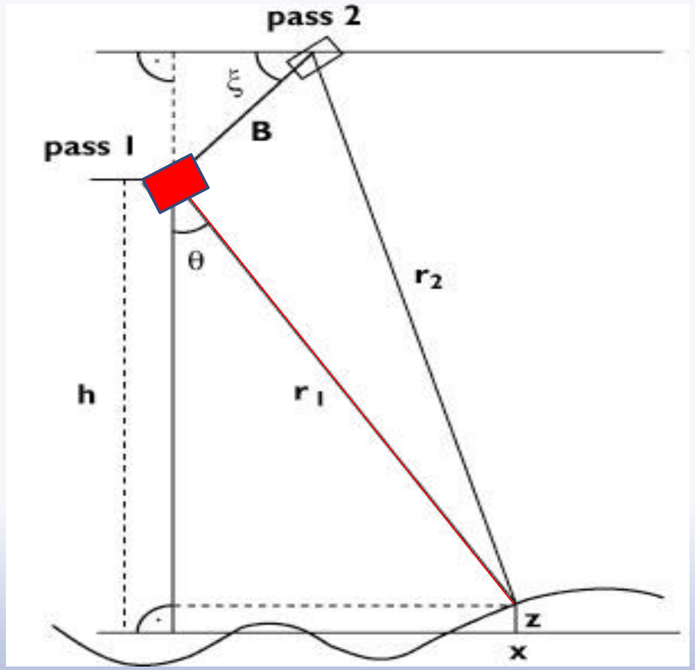

L. Charrier, B. Scheuchl, J. Mouginot, S. Jeong, V. Brancato, E. Rignot

InSAR method

SAR $$\phi = \frac{4\pi}{\lambda} r_1 + \phi_{ground} + \phi_{noise}\ [2\pi]$$

InSAR $$\Delta\phi = \frac{4\pi}{\lambda}\left(r_1 - r_2 + \phi_{noise\ 1} - \phi_{noise\ 2}\right)\ [2\pi]$$

$$\Delta\phi = \Delta\phi_{\ atmosphere} + \Delta\phi_{\ imaging\ geometry} + \Delta\phi_{\ topography} + \Delta\phi_{\ surface\ deformation}$$

$$\Delta\phi_{\ glacier\ flow\ motion}$$

$$\Delta\phi_{\ tidal\ motion}$$

InSAR method

SAR $\phi = \frac{4\pi}{\lambda} r_1 + \phi_{ground} + \phi_{noise}\ [2\pi]$

InSAR $\Delta\phi = \frac{4\pi}{\lambda}\left(r_1 - r_2 + \cancel{\phi_{ground}}_1 - \cancel{\phi_{ground}}_2 + \phi_{noise\ 1} - \phi_{noise\ 2}\right)\ [2\pi]$

$$\Delta\phi = \cancel{\Delta\phi_{\ atmosphere}} + \cancel{\Delta\phi_{\ imaging\ geometry}} + \cancel{\Delta\phi_{\ topography}} + \Delta\phi_{\ surface\ deformation}$$

Neglected

Removed

$\Delta\phi_{\ glacier\ flow\ motion}$

$\Delta\phi_{\ tidal\ motion}$

Double difference interferometry

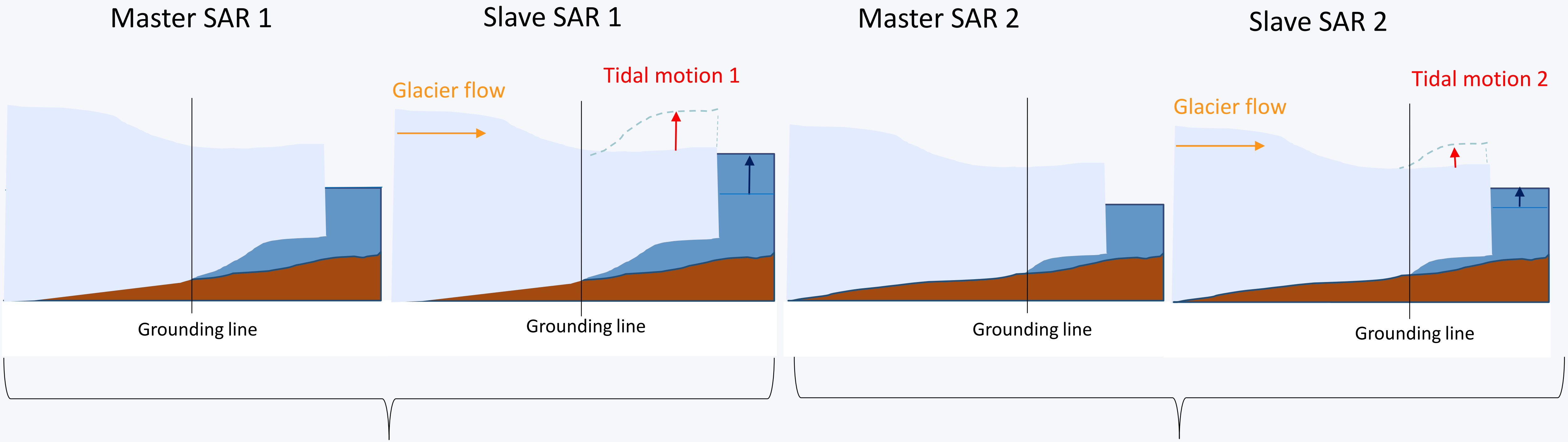

Interferogram 1
Glacier flow
Tidal motion 1

Interferogram 2
Glacier flow
Tidal motion 2

Interferogram 1 - Interferogram 2
Tidal motion 1 - Tidal motion 2

L. Charrier, B. Scheuchl, J. Mouginot, S. Jeong, V. Brancato, E. Rignot

Grounding line: the upstream limit of detection of vertical motion

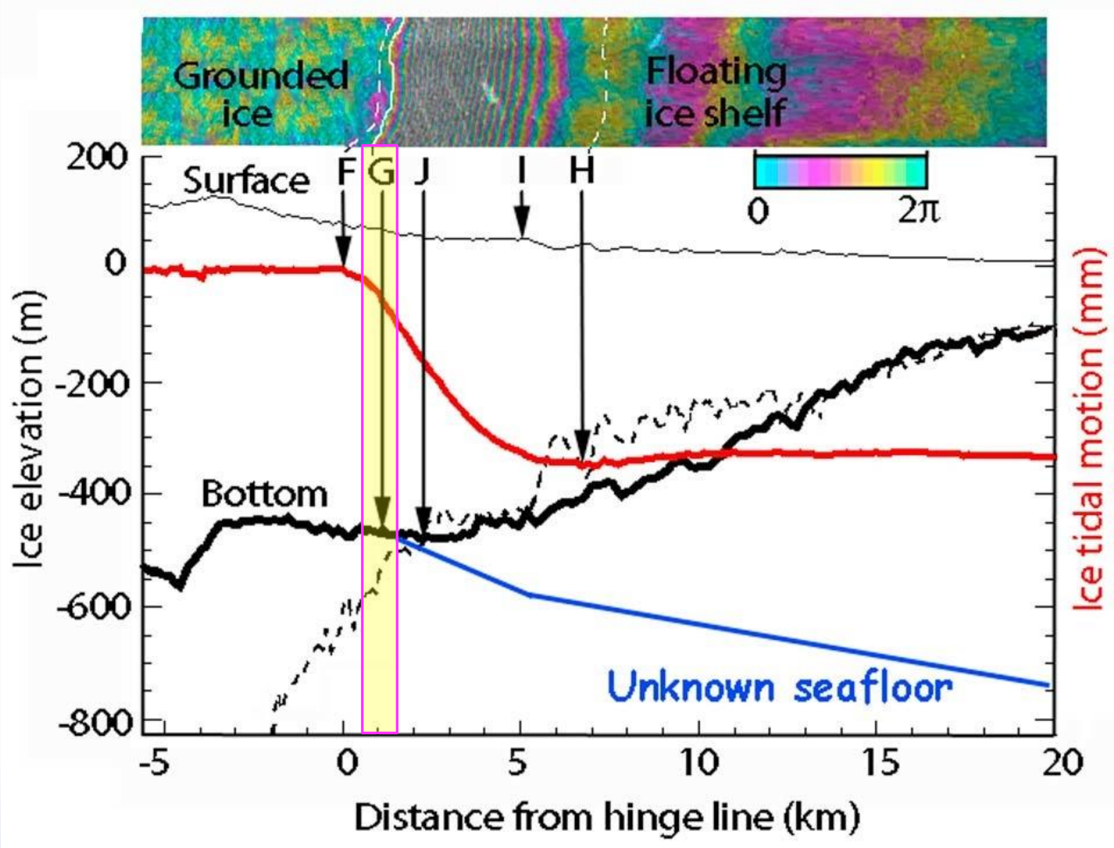

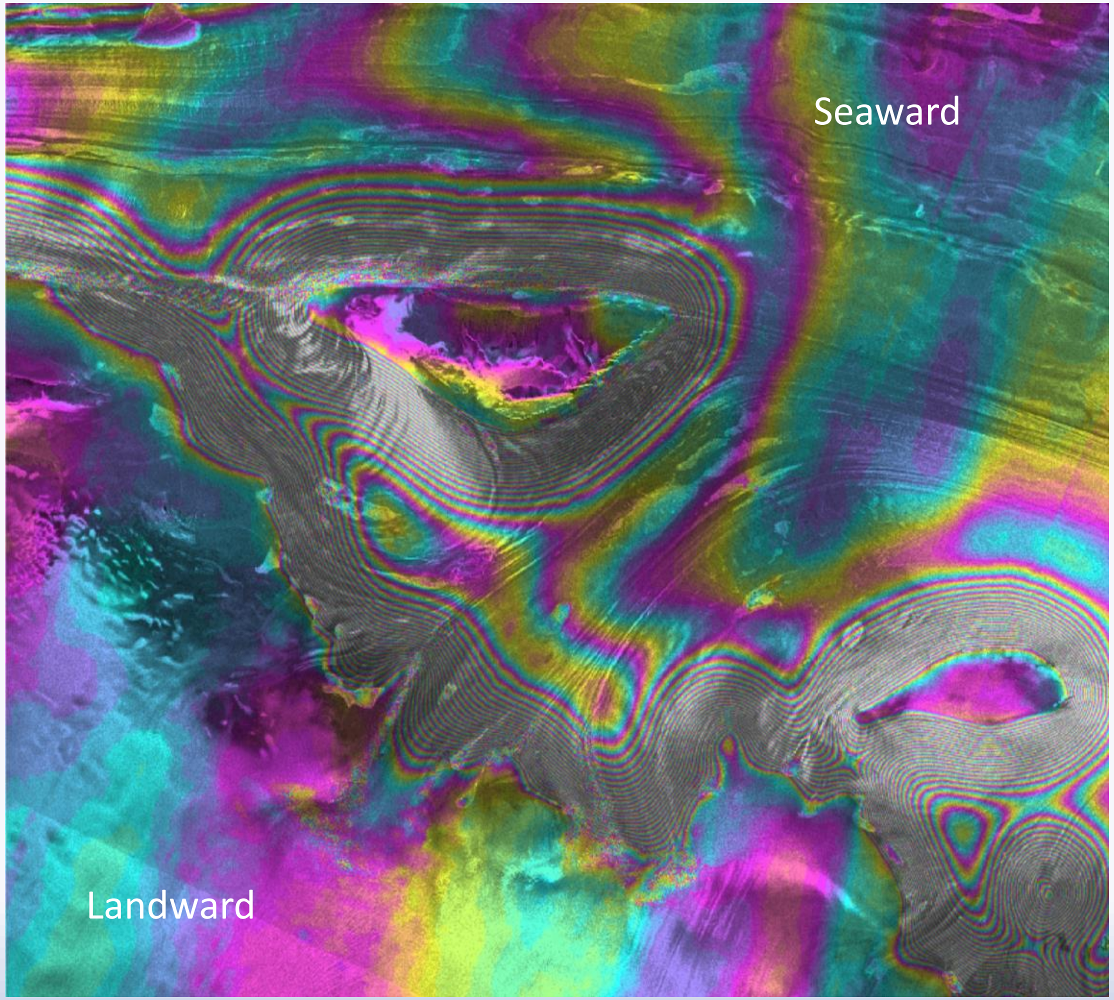

DInSAR image

L. Charrier, B. Scheuchl, J. Mouginot, S. Jeong, V. Brancato, E. Rignot

Grounding line: the upstream limit of detection of vertical motion

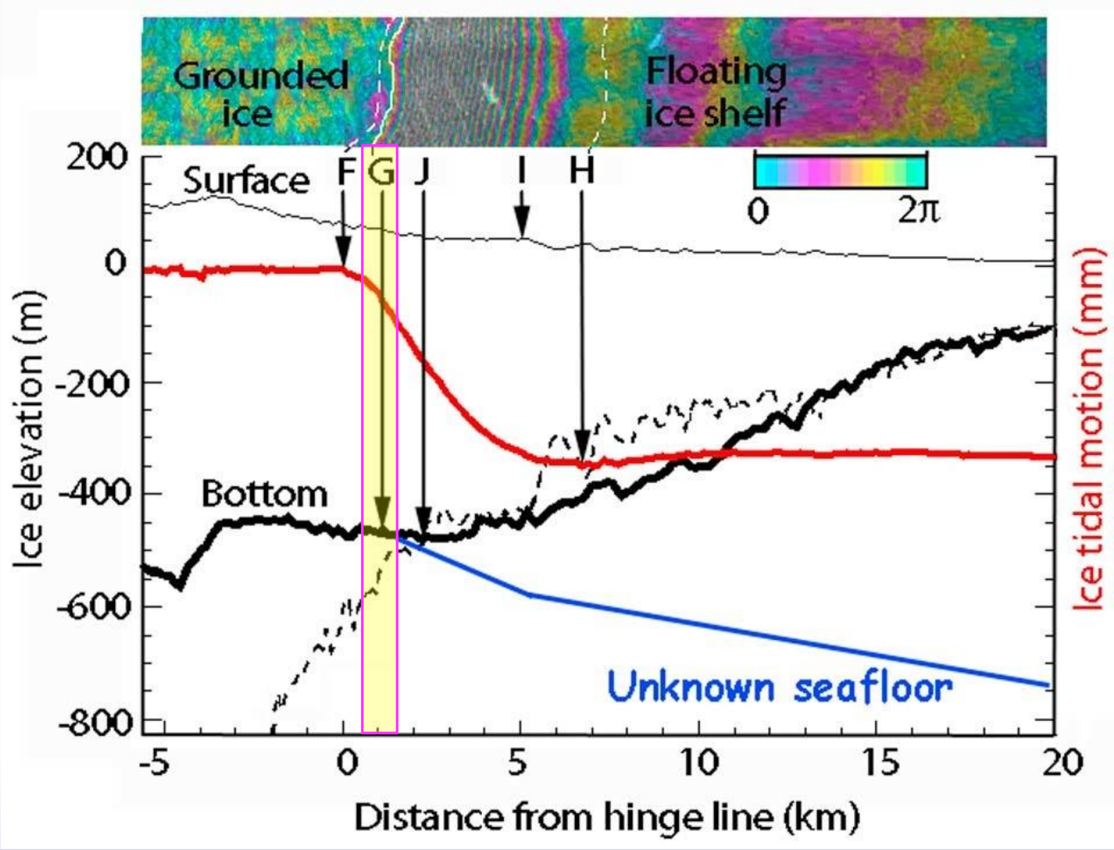

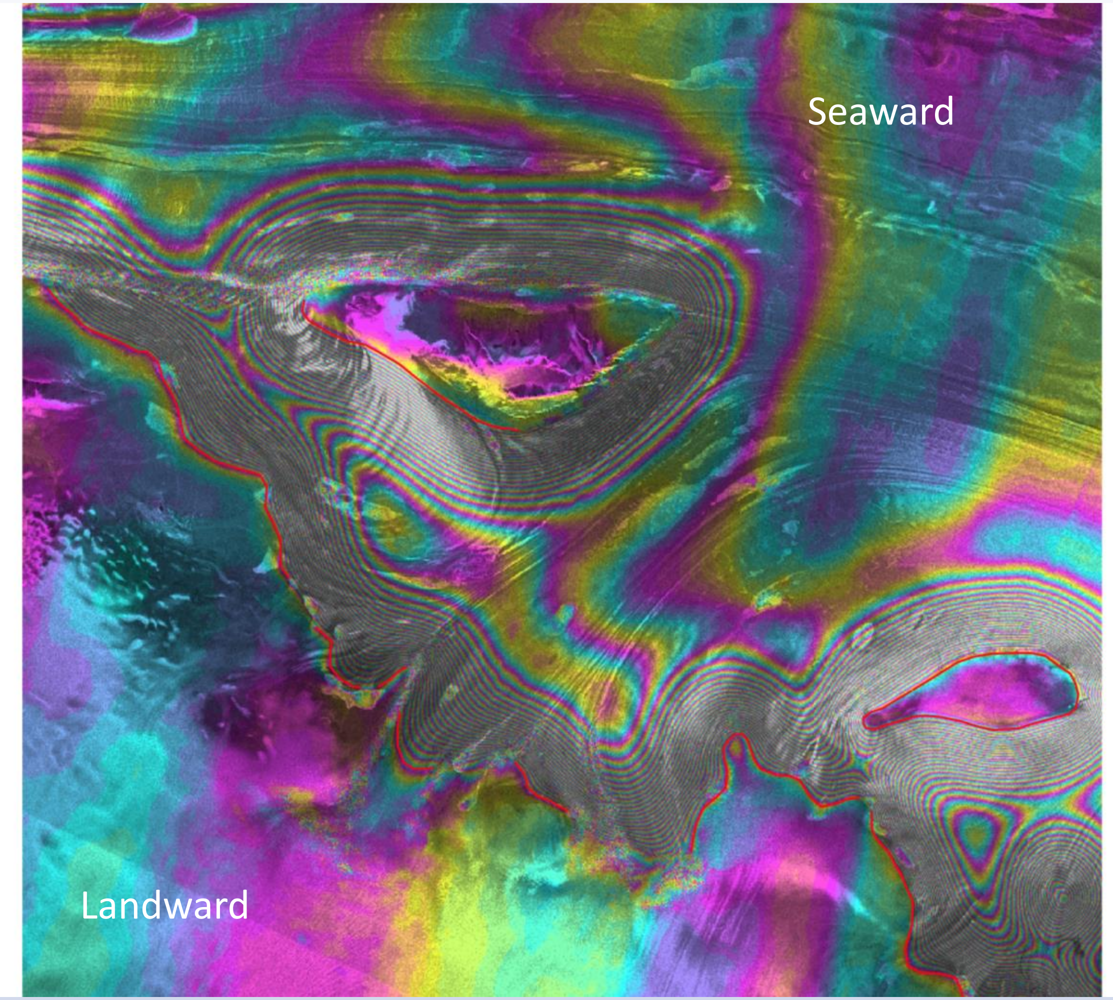

DInSAR image

L. Charrier, B. Scheuchl, J. Mouginot, S. Jeong, V. Brancato, E. Rignot

Grounding Zone Width

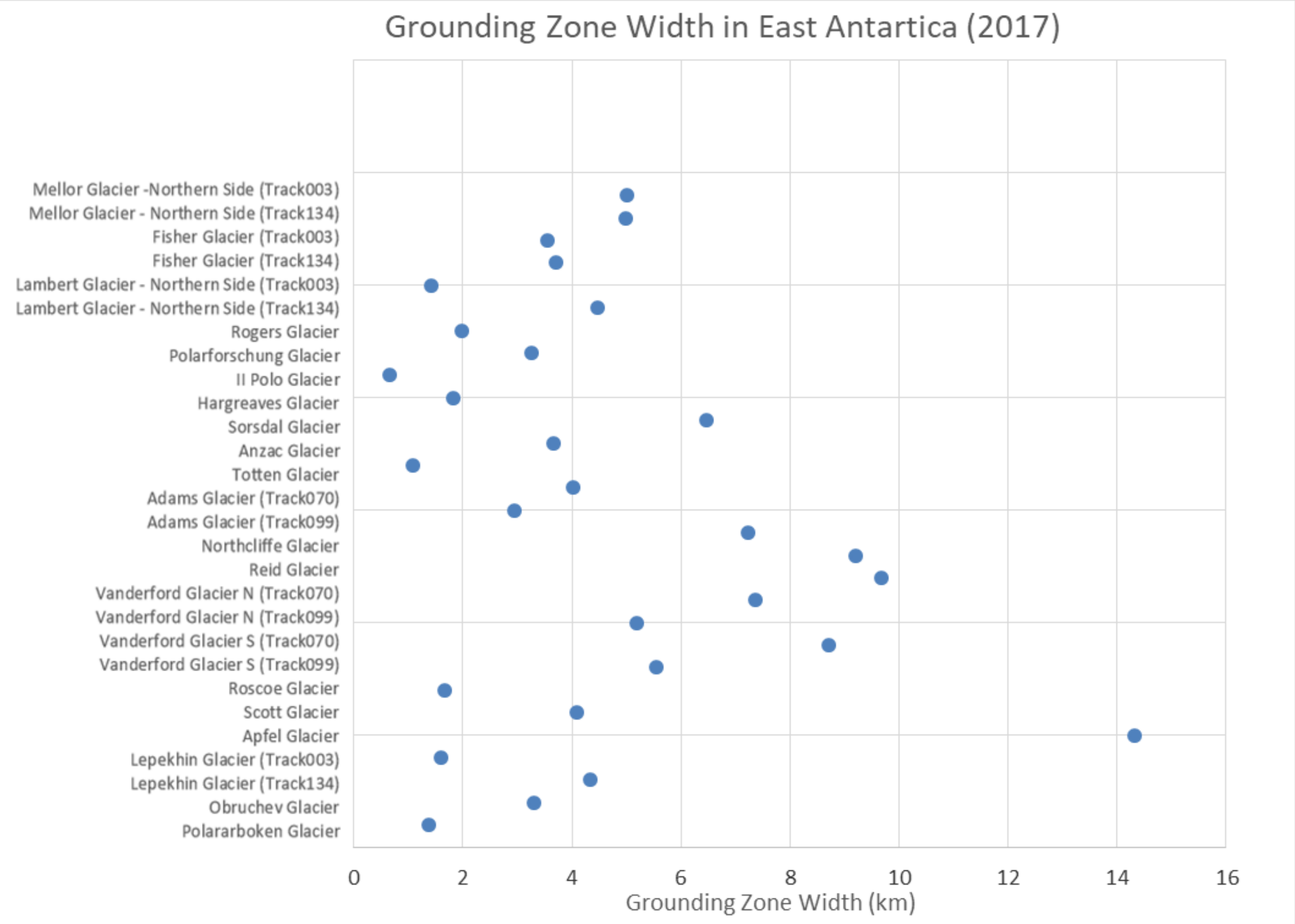

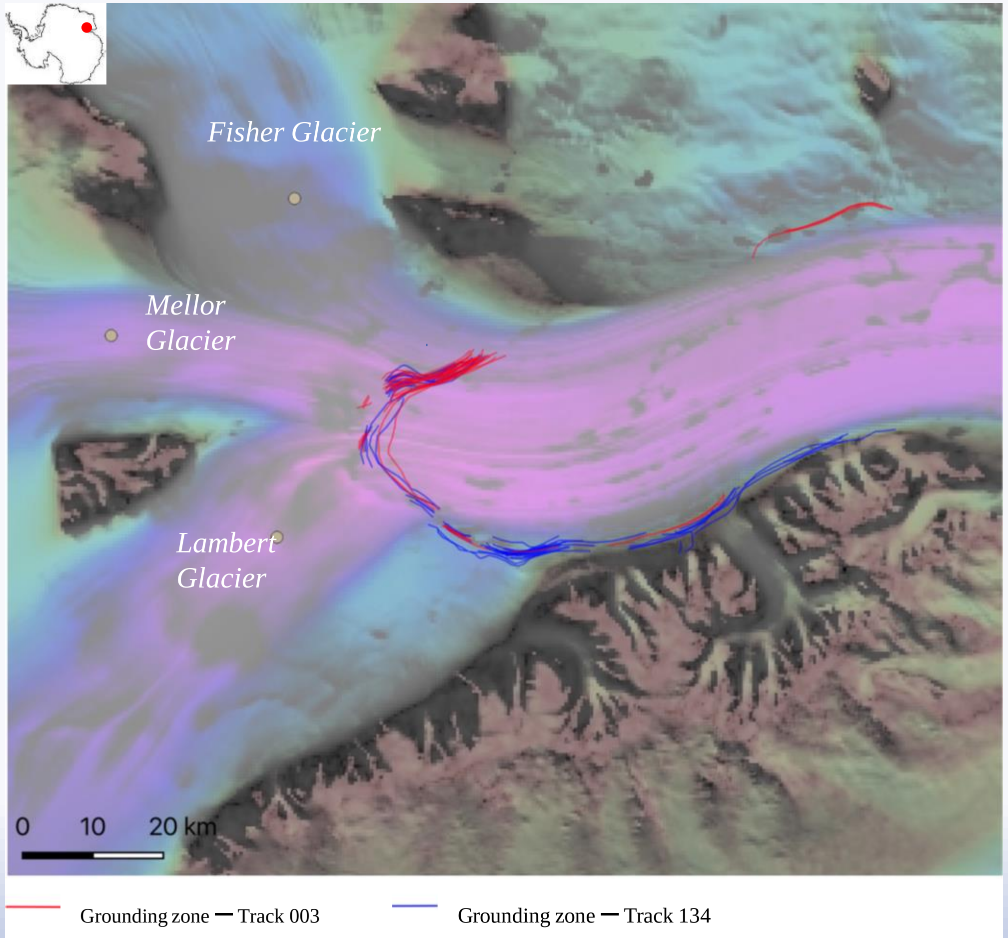

Influence of the maximum of tidal displacement

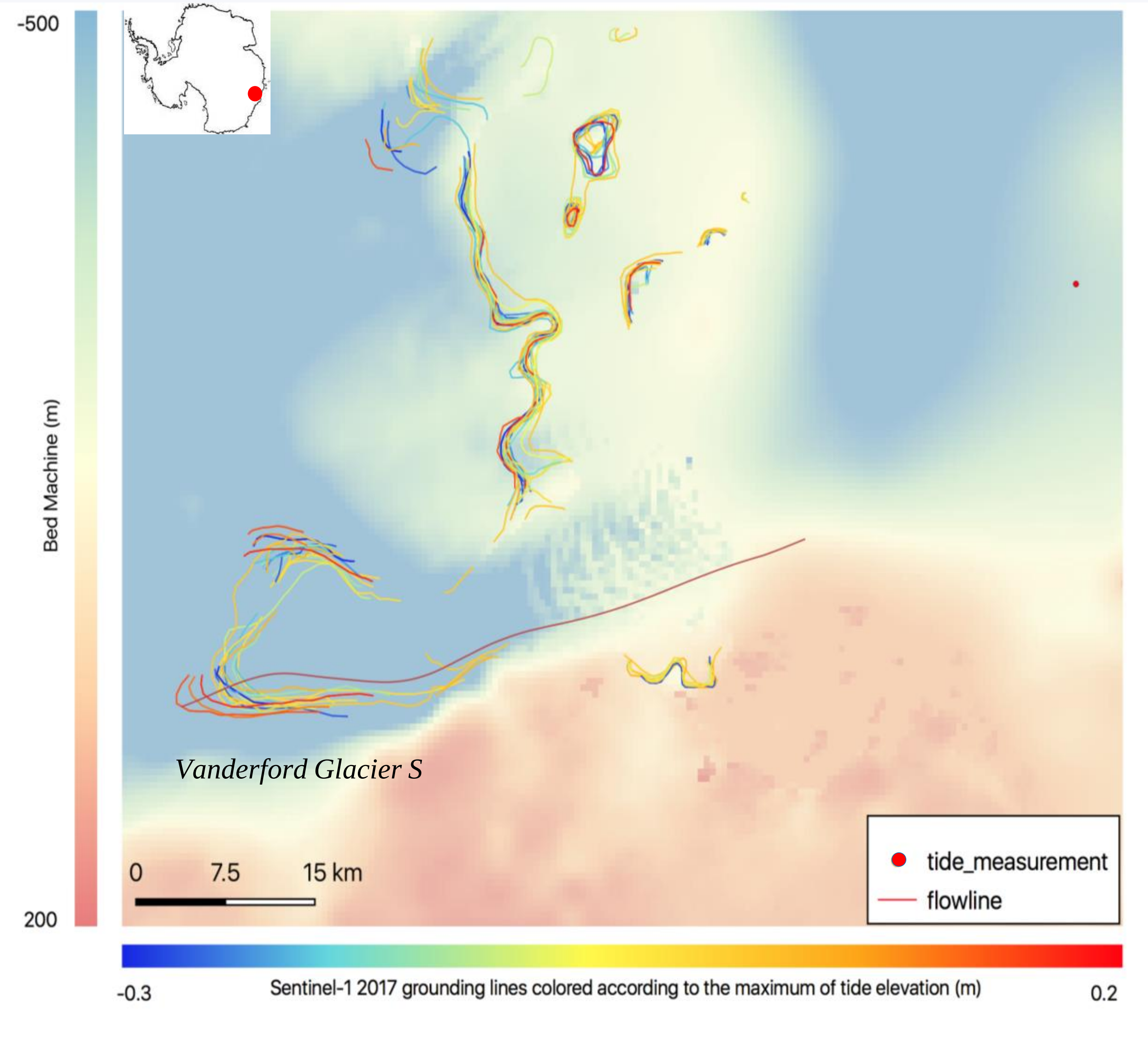

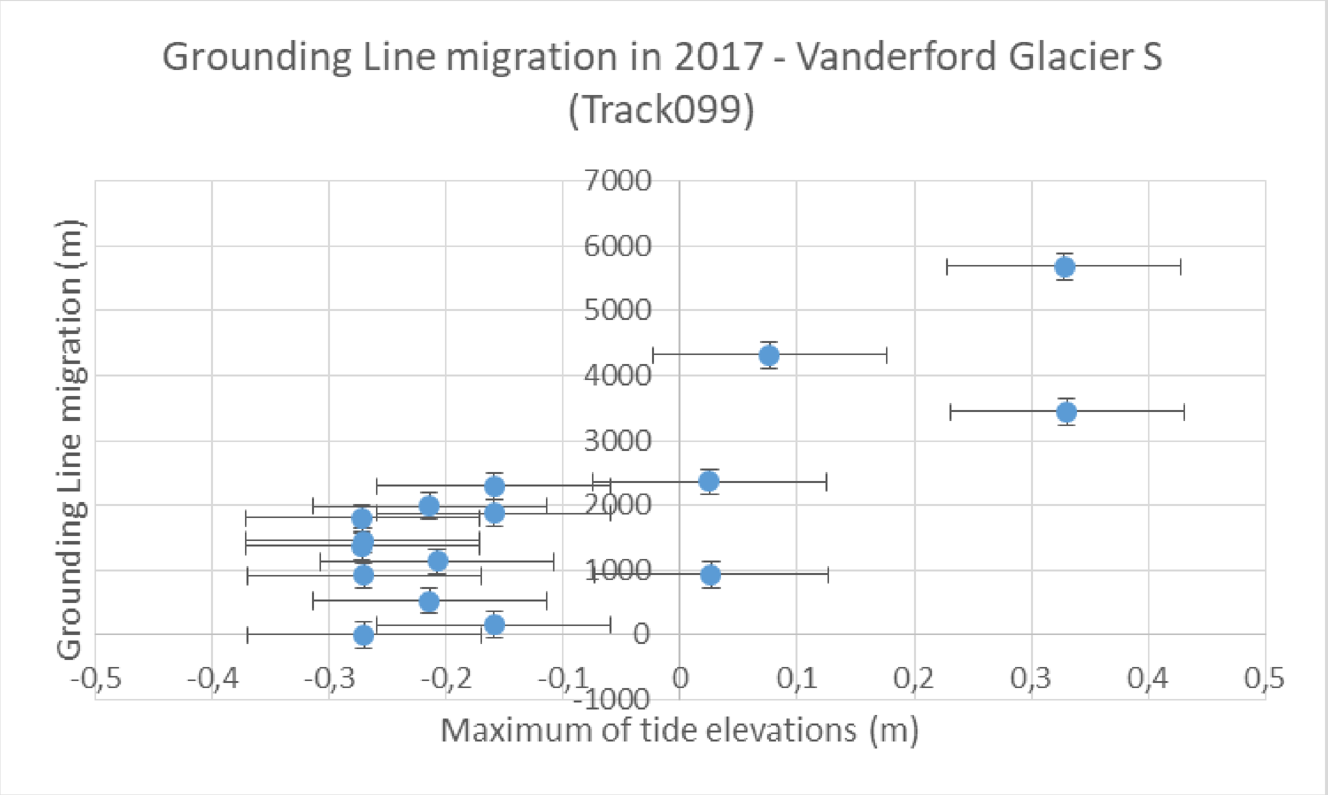

Sentinel-1 2017 (Track099) GL migration along the center flow line of Southern part of Vanderford Glacier compared with the maximum of tide elevations computed with tide model CAT2008A (Padman et al,, 2002)

Influence of the maximum of tide elevation

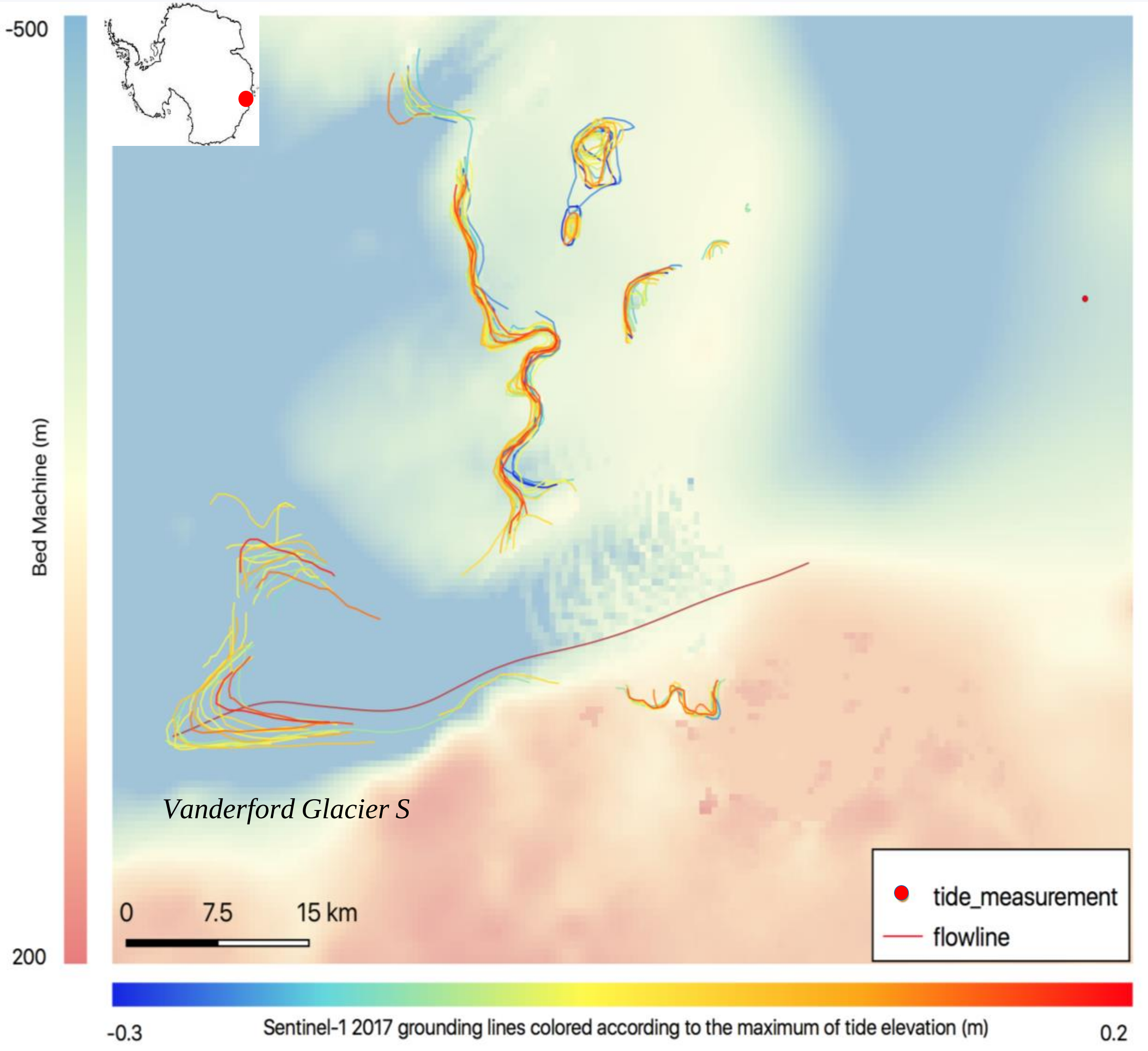

=> Tide cycle may play a role

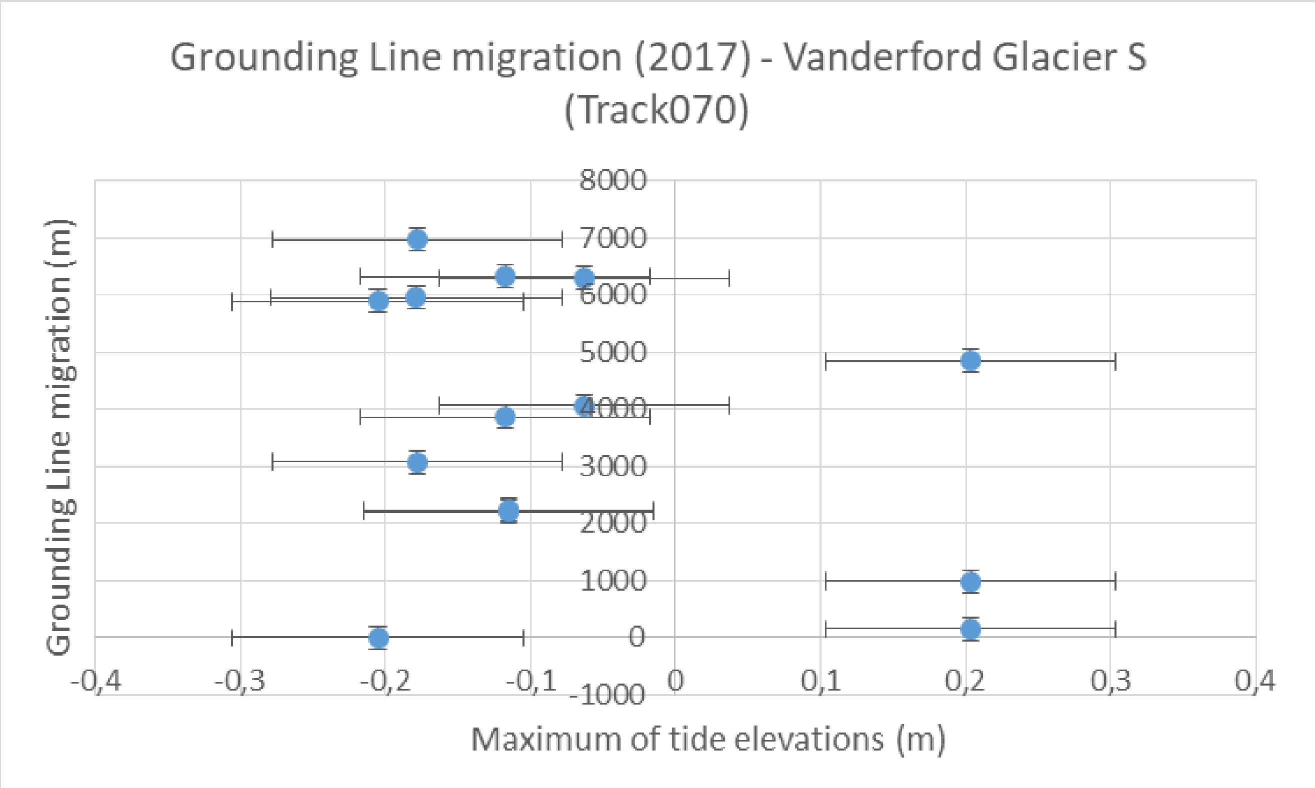

Sentinel-1 2017 (Track099) GL migration along the center flow line of Southern part of Vanderford Glacier compared with the maximum of tide elevations computed with tide model CAT2008A (Padman et al,, 2002)

Influence of the bed topography

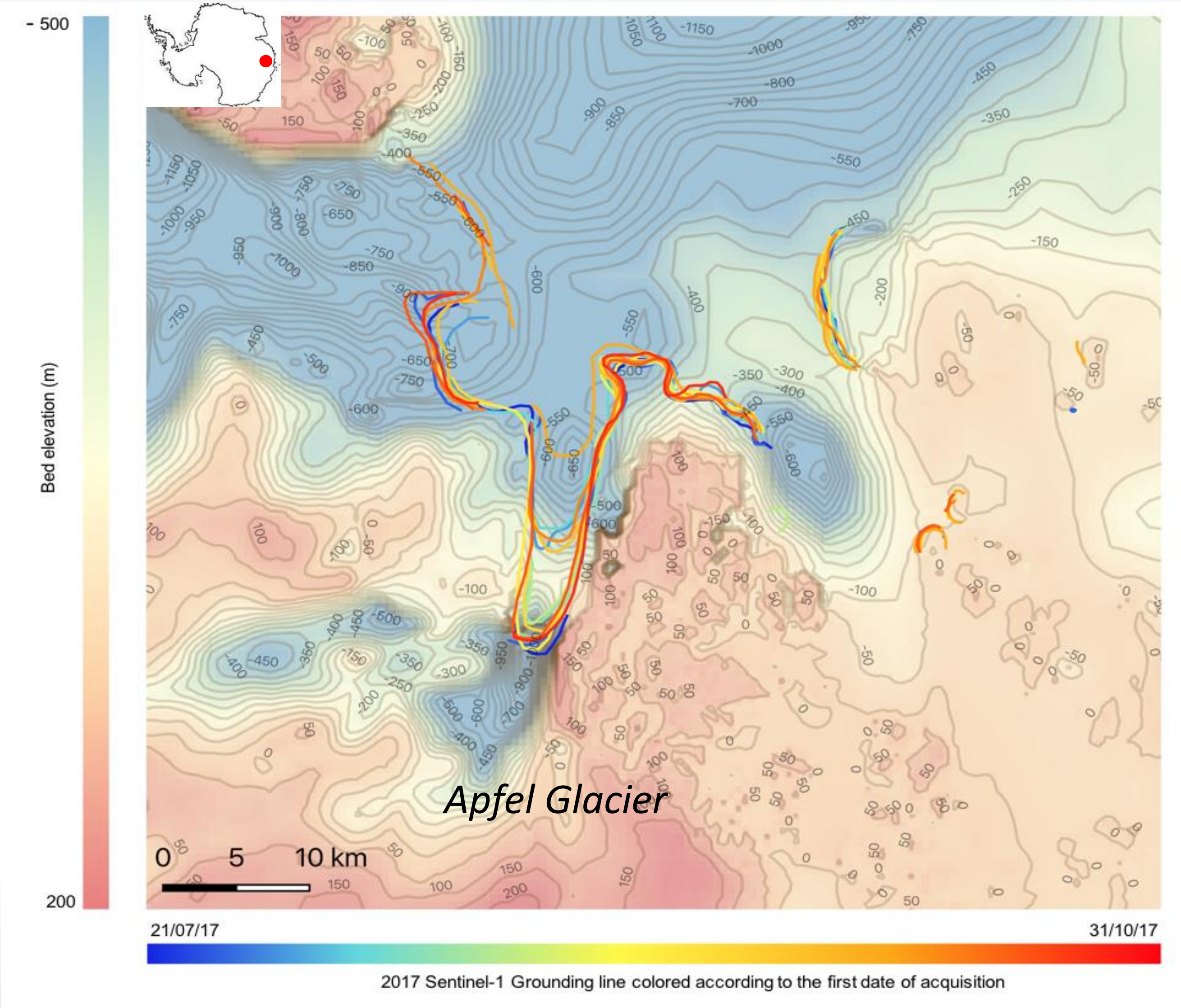

Grounding line migration compared to the bed topography model from Morlighem, 2019 (in review)).

Comparison with previous years

Grounding lines mapped for the first time over 250 km of coast

=> Position with GL used by the model was not suitable

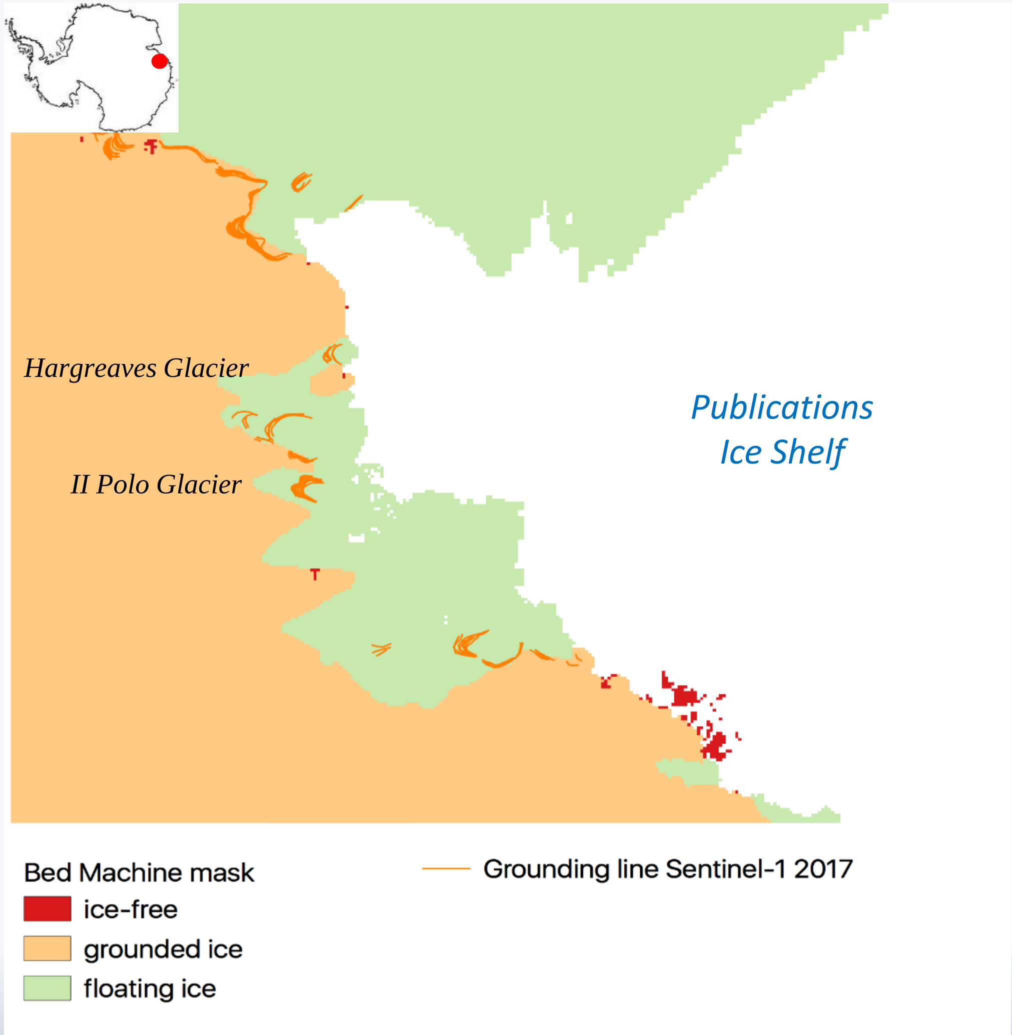

Bed topography model from Morlighem, 2019 (in review)

Slight advance of grounding lines between 1996 and 2017

Advance of 4 km near Lambert Glacier
Along a prograde bed

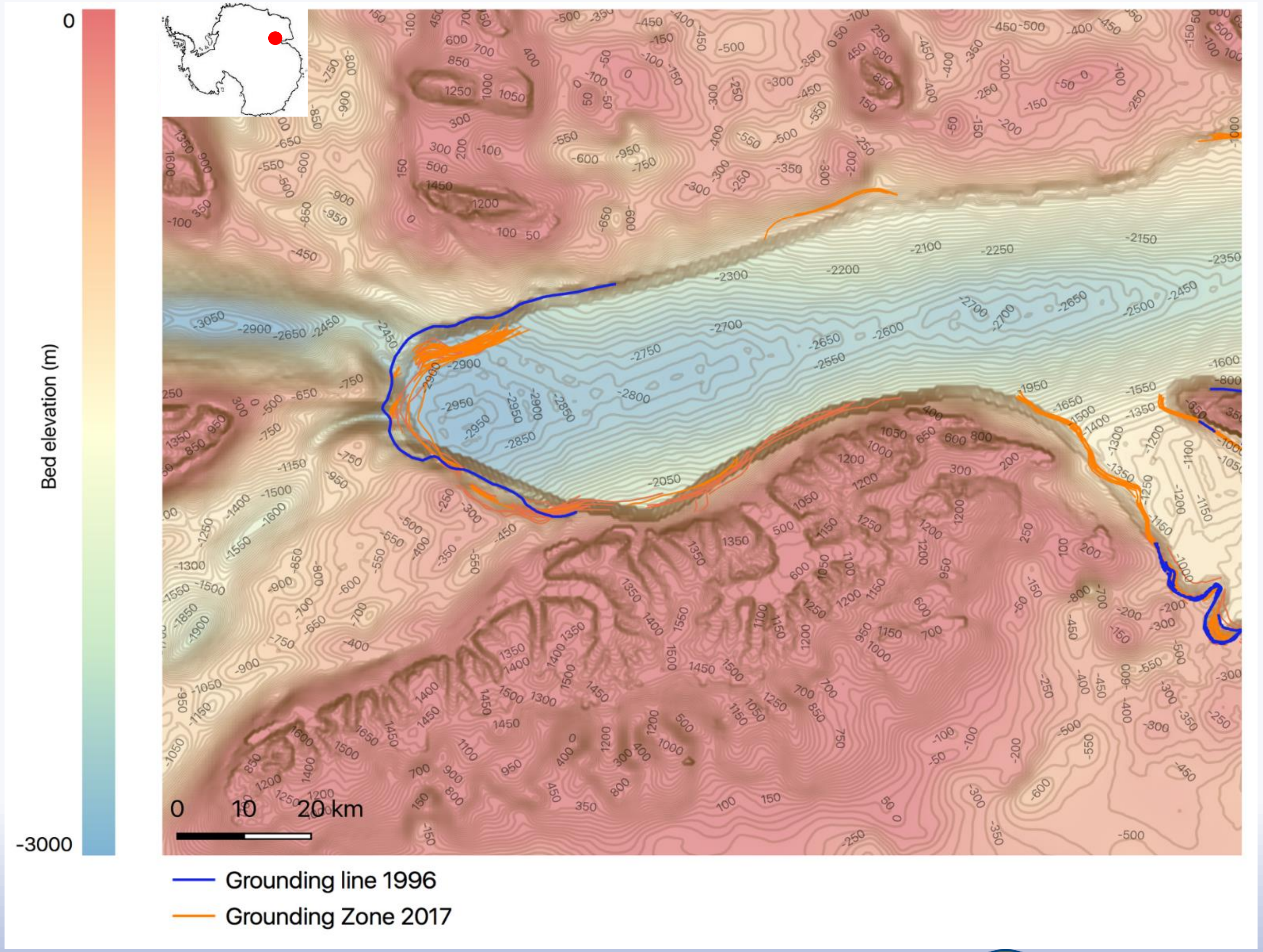

Strong retreat of grounding lines between 1996 and 2017

Retreat of 20 km near Vanderford Glacier
Along a retrograde bed

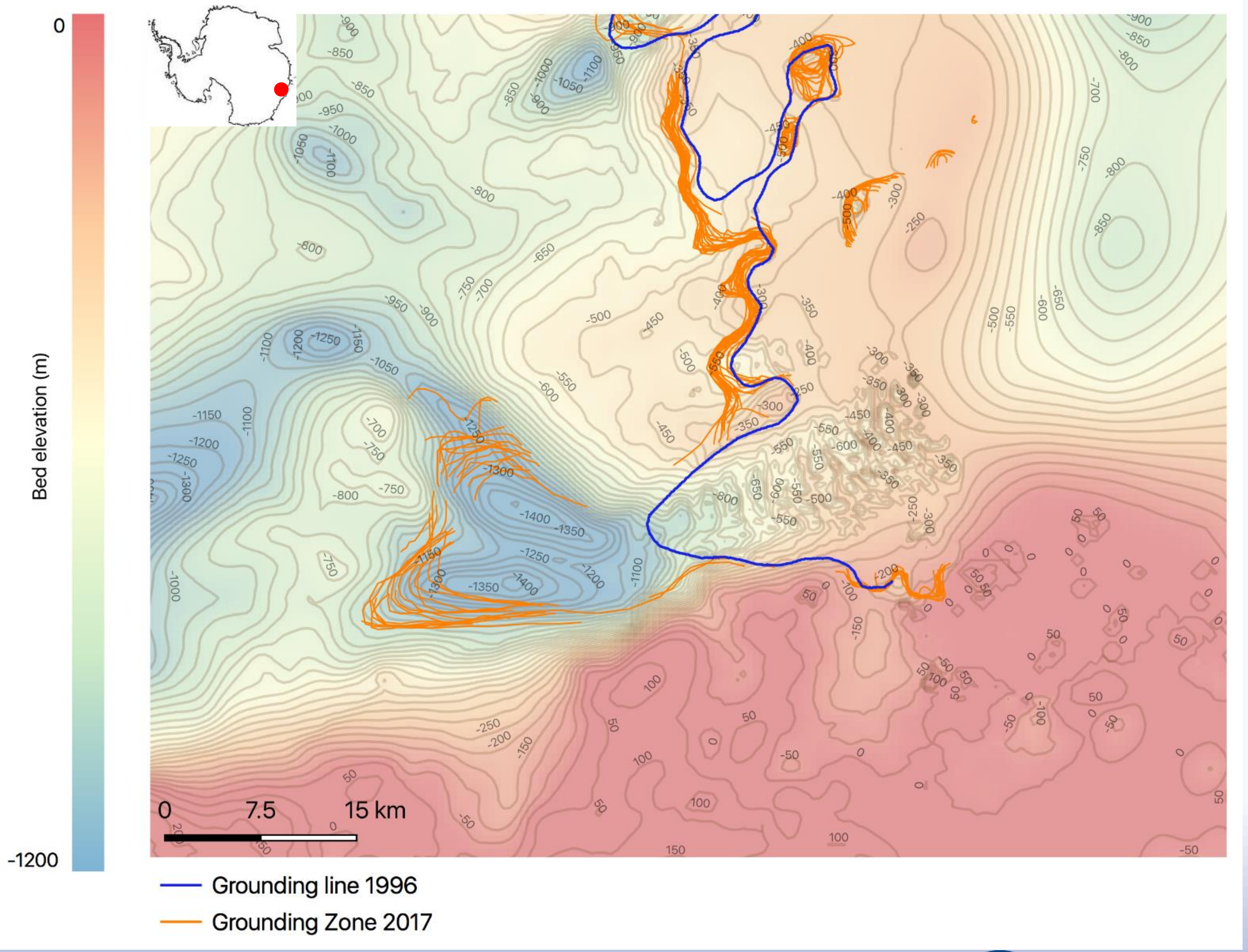

Conclusion

➢ **Short-term variations**

Moving position of the grounding line (variations from 0.4 km to 14.3 km)

$\Rightarrow$ But not yet implemented in numerical models

➢ **Long-term variations**

- Areas where no grounding lines were mapped before : new information for numerical models
- Short-term migration has to be taken into account
- Huge retreat in some areas and slight advances in others

➢ **To explain short-term variations**

Parameters involved in grounding line migration:

- Bed topography
- Tide elevation: The tidal flushing may play a role (further investigations needed)
  The tide cycle also may play a role (further investigations needed)

Comparison with predicted grounding line migration:

the bed should have visco-elastic properties (Sayag et al., 2017)

Perspective

- **Expansion of the Grounding Zone measurement to the entire coastline of Antarctica**

- **Quantitative evaluation of Grounding Line migration (short and long term) for more glaciers**

L. Charrier, B. Scheuchl, J. Mouginot, S. Jeong, V. Brancato, E. Rignot

Acknowledgement

I am very gratfull to Eric Rignot, Bernd Scheuchl, Virginia Brancato, Seongsu Jeong, Jérémie Mouginot and Mathieu Morlighem

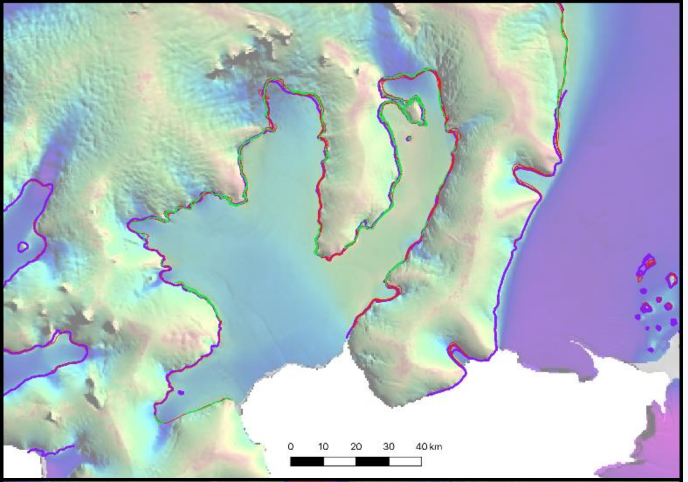

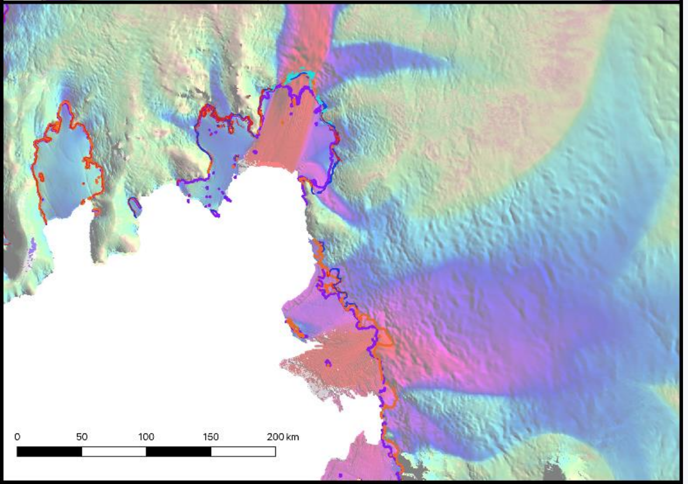

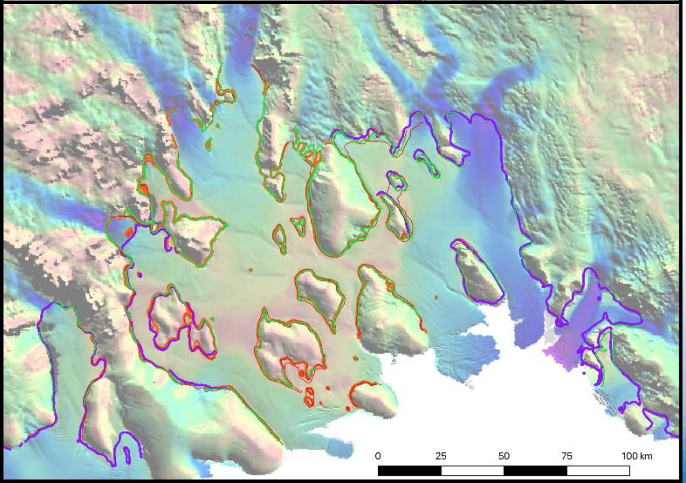

Thank you for your attention !

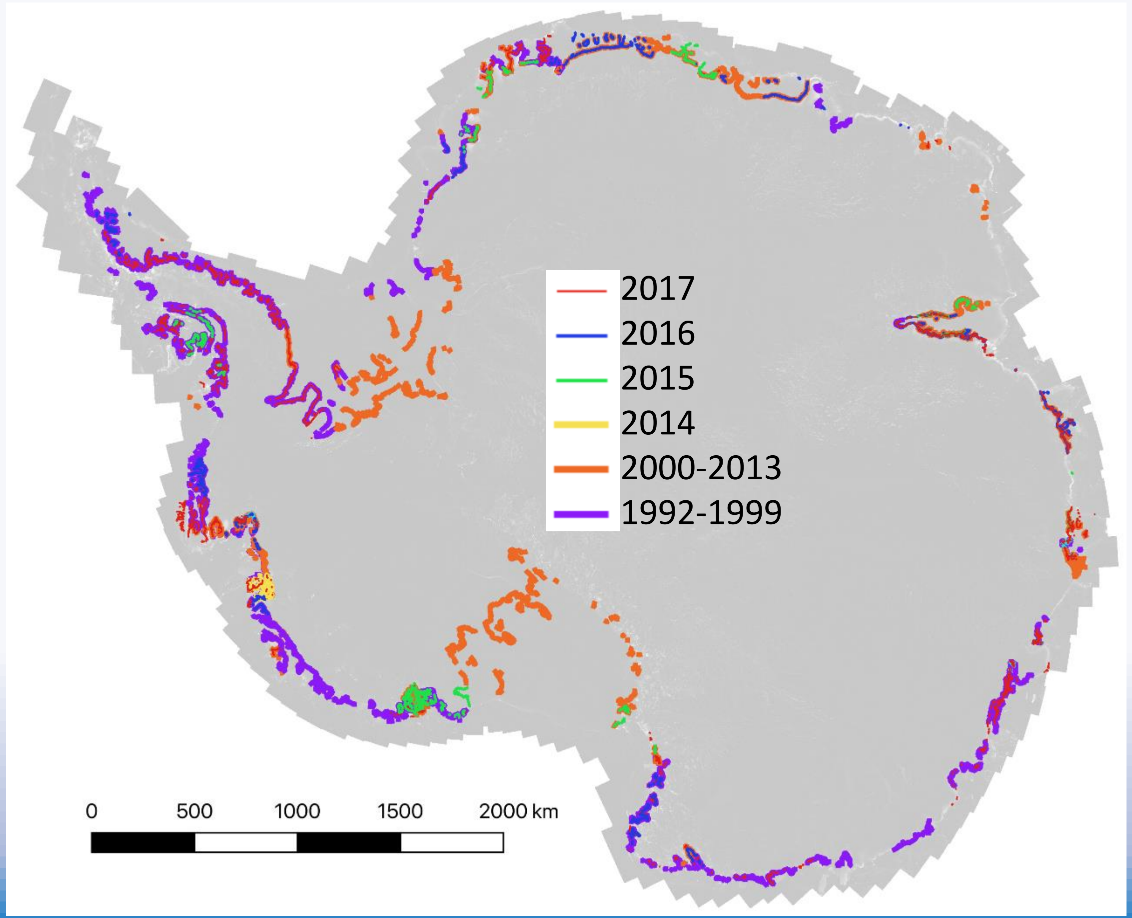

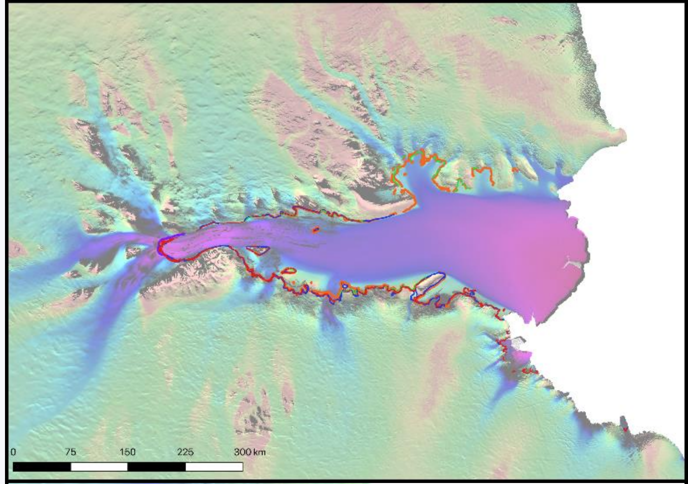

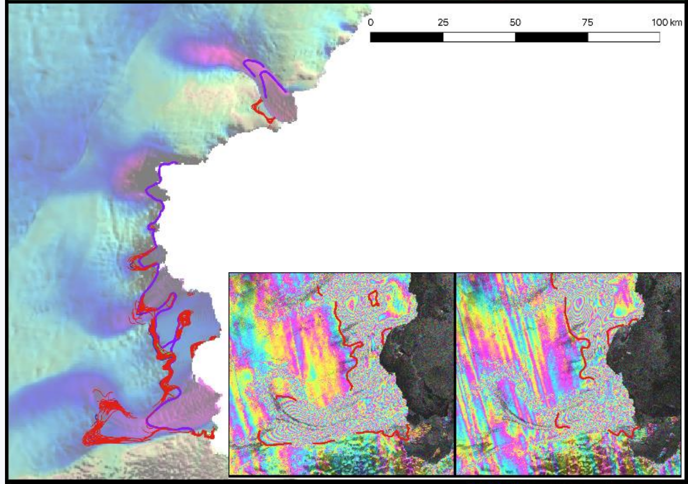

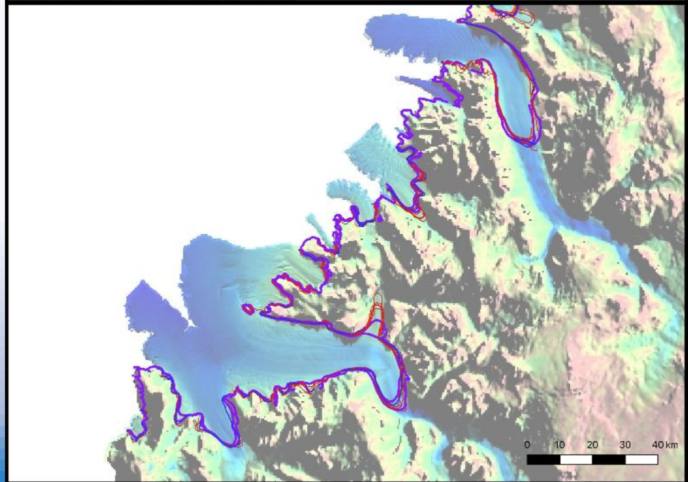

References

Bamber, J. L., Oppenheimer, M., Kopp, R. E., Aspinall, W. P. & Cooke, R. M. Ice sheet contributions to future sea-level rise from structured expert judgment. *Proc Natl Acad Sci USA* **116**, 11195–11200 (2019).

Padman, L., Fricker, H. A., Coleman, R., Howard, S. & Erofeeva, L. A new tide model for the Antarctic ice shelves and seas. Ann. Glaciol 34, 247–254 (2002).

Sayag, R. & Worster, M. G. Elastic dynamics and tidal migration of grounding lines modify subglacial lubrication and melting: tidal migration of grounding lines. *Geophys. Res. Lett.* **40**, 5877–5881 (2013).

Thomas, R., Rignot, E., Kanagaratnam, P., Krabill, W. & Casassa, G. Force-perturbation analysis of Pine Island Glacier, Antarctica, suggests cause for recent acceleration. *Ann. Glaciol.* **39**, 133–138 (2004).

Implication for the bed stiffness

Model for a hard bed: *Thomas and Bentley, 1978*

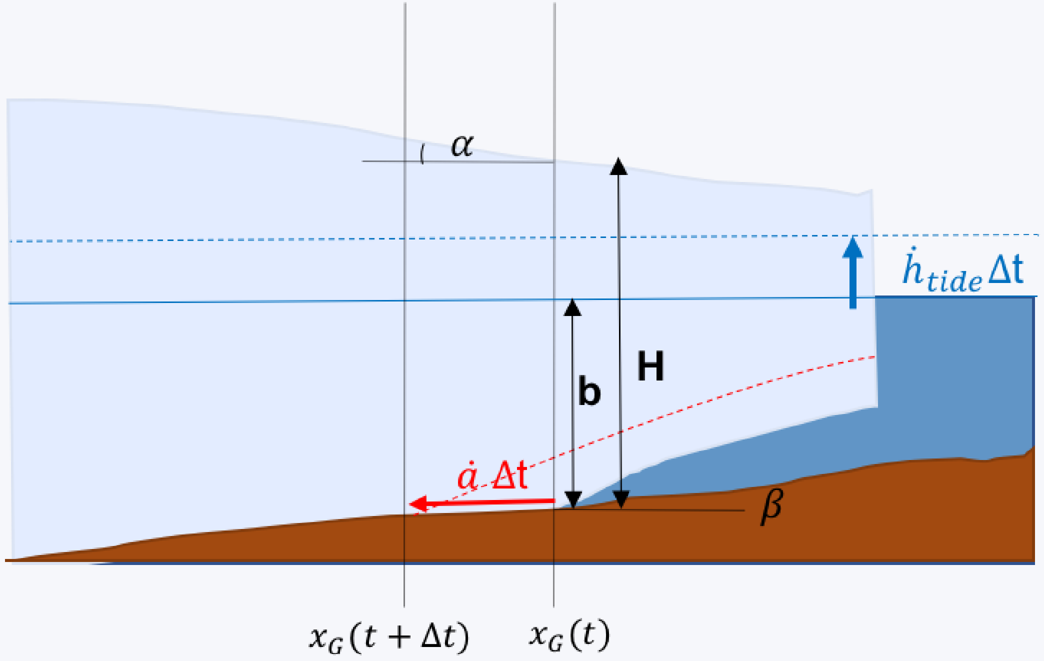

Predicted migration: $\dot{a} = \dfrac{\dot{h}_{tide}\frac{\rho_w}{\rho_i}}{\alpha - \beta\frac{1-\rho_w}{\rho_i}}$

	Vanderford Glacier S	Vanderford Glacier N	Anzac Glacier
Migration for a tide rise of 1 m (m) (Thomas and Bentley, 1978)	-79	-93	-97
Oberved migration landward (m)	-4557	-690	-900
Oberved migration seaward (m)	4159	6684	1034

=> Visco-elastic properties of the bed

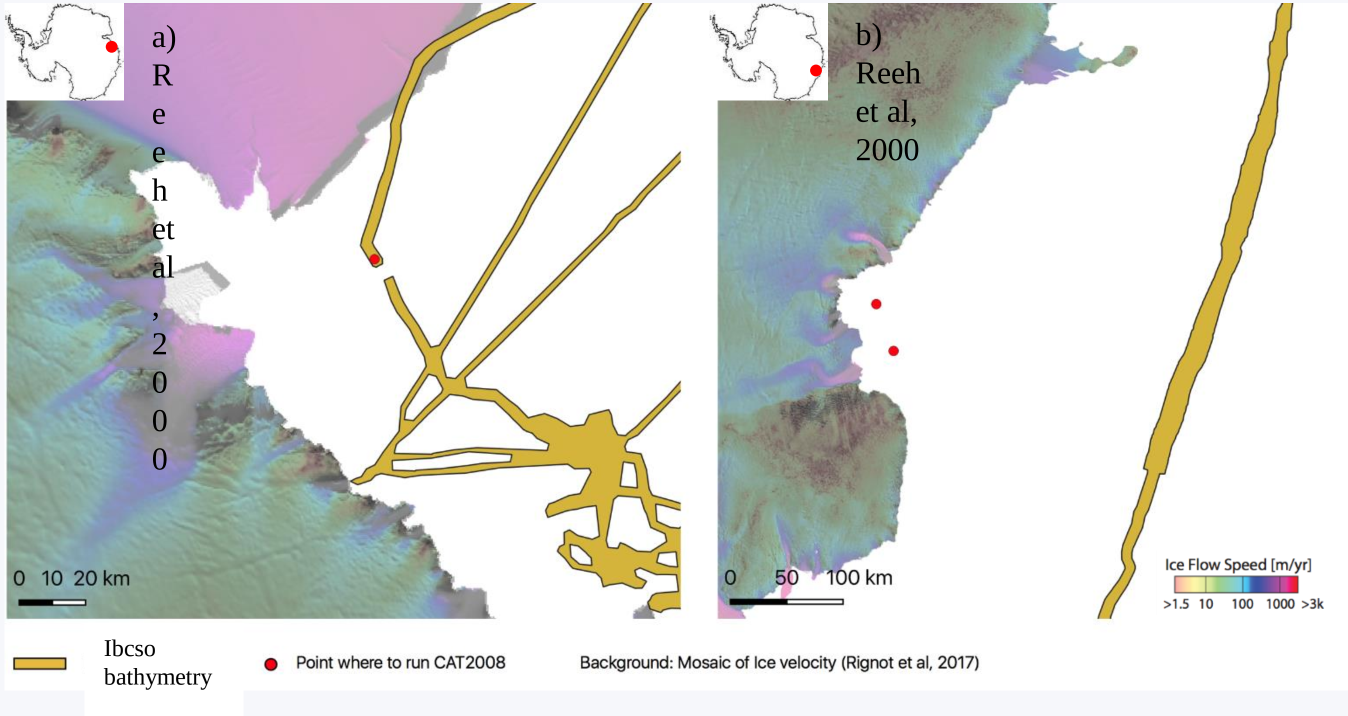

Figure 11 Localization of tide model computation a) around Publications Ice Shelf b) around Vanderford glacier. The background is a velocity map produced by Rignot's group [Mouginot et al., 2019 (in review)]

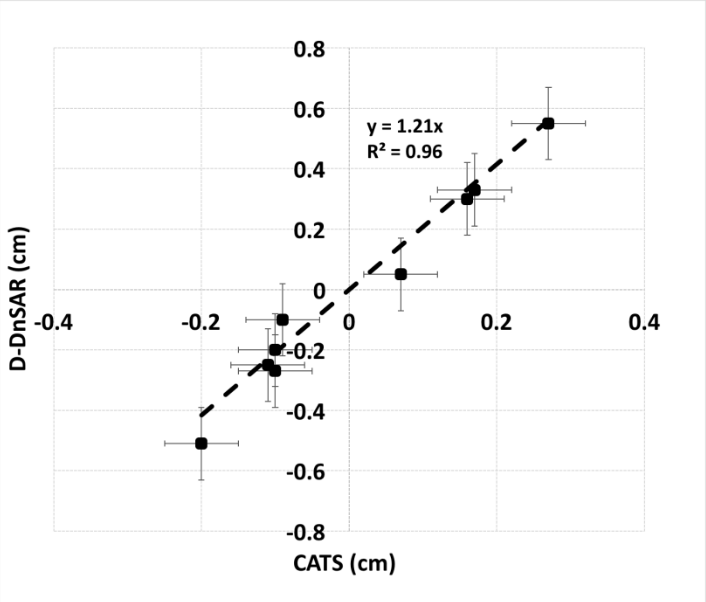

Figure 7 Comparison between the CSK DInSAR recorded vertical differential tidal displacements along the main trunk of Pine Glacier, West Antarctica and the corresponding estimates from the CATS2.01 tidal model at a center location of 73.761629 South and 104.803 West (Padman et al., 2002).